

# Dynamic Behavior of Photoinduced Birefringence of Copolymers Containing Aminonitro Azobenzene Chromophore in the Side Chain

Dong Hoon Choi\* and Suk Hoon Kang

College of Environment and Applied Chemistry, Institute of Material Science and Technology,  
I.L.R.I, Kyung Hee University, Yongin-shi, Kyungki-do 449-701, Korea

Received July 1, 1999

Photoresponsive side chain polymers containing aminonitro azobenzene were synthesized for studying optically induced birefringence. Four different copolymers were prepared using methacrylate,  $\alpha$ -methylstyrene, and itaconate monomer. Two copolymers are totally amorphous and the other two are liquid crystalline in nature. Trans-to-cis photoisomerization was observed under the exposure of UV light with UV-VIS absorption spectroscopy. Reorientation of polar azobenzene molecules induced optical anisotropy under a linearly polarized light at 532 nm. The dynamic parameters of optically induced birefringence let us compare the effect of polymeric structure on the rate of growth and decay of the birefringence. Besides the effect of glass transition temperature on the dynamics of photoinduced birefringence, we focused our interests on the geometrical hindrance of polar azobenzene molecules and cooperative motion of environmental mesogenic molecules in the vicinity of polar azobenzene moiety.

## Introduction

There is a considerable interest in the synthesis and characterization of azobenzene containing polymers for several reasons as these materials to possess unique optical properties.<sup>1-5</sup> In addition to the studies in the direction of nonlinear optical properties, there is constantly increasing attention in the field of optical data storage and holographic applications. Optically induced anisotropy is a very promising property for optical information storage and erasing. The mechanism of writing information involves photoinduced excitation of the azobenzene group, which undergoes *trans-cis-trans* isomerization. This phenomenon is attributed to photoinduced birefringence that results from reorientation of azobenzene molecules.

The photoinduced *trans-cis* isomerization of azobenzene and its derivatives has been studied in amorphous and liquid crystalline polymers.<sup>6,7</sup> The type of optically induced isomerization is also of particular interest because the induced changes in molecular orientation of azobenzene moiety can affect the surrounding molecules. In addition, the induced birefringence and dichroism that result from molecular reorientation could potentially be used to investigate the polymer property and environment in the vicinity of the polar azobenzene molecules.

In the guest-host system, azobenzene guest molecules exist in their lower energy, *trans* form, and are randomly oriented throughout the film. If the polymer film is then subjected to a linearly polarized light of an appropriate wavelength, the azobenzene moieties that have a nonvanishing transition dipole ( $\Delta\mu$ ) component in the polarization direction of the pump beam can be photoisomerized to the *cis* form. Through a thermal effect or exposure to light, some molecules in the *cis* form can revert to the *trans* form, although a given molecule may not be necessarily converted to the ini-

tial molecular orientation. After several repetitive photoexcitation and isomerization cycles, an excess of azobenzene moiety with transition dipole moments perpendicular to the polarization direction of the excitation light can be stabilized to new molecular direction. The azobenzene molecules placed in the perpendicular direction of polarization of pump light cannot interact with the excitation light and therefore become inert to the pump beam. The polymer matrix that was isotropic becomes anisotropic after irradiation under the excitation light. This behavior can be observed both in amorphous and liquid crystalline polymers. The anisotropic polar molecular distribution gives rise to birefringence and dichroism in the film.

Usually, the induced birefringence increases under the light at the wavelength of absorption. Without light, the birefringence will relax either fast or slow, which depends on the polymer structure. Finally, we can remove the birefringence under a circularly polarized light to randomize the orientation of azobenzene moieties. The time required to reach maximum birefringence is expected to depend on the structure, polarity, environment of azobenzene moieties, the thickness of the film, the wavelength of the excitation light, and intensity. Additionally, the photoinduced birefringence is related to the structure of azo chromophore, the type of the polymer backbone, and the interaction between azobenzene dipoles. Natansohn *et al.* have recently performed a number of studies on how such factors affect the dynamics of the photoinduced orientation of azobenzene moiety.<sup>8-12</sup>

In this study, we synthesized four different types of copolymer bearing the same aminonitro azobenzene moiety in the side chain. We investigated the growth and decay of the induced birefringence in the copolymer film. Among many factors to affect the dynamics of the photoinduced birefringence, we performed the study on the effects of environment of azobenzene moieties and intensity of excitation light on

the birefringence.

### Experimental Section

**Materials.** 4-hydroxybenzoic acid, 6-chloro-1-hexanol, triphenylphosphine, diisopropyl azodicarboxylate (DIAD), methacryloyl chloride, itaconic acid, azobisisobutyronitrile (AIBN), disperse red 1, *m*-isopropenyl- $\alpha,\alpha$ -dimethylbenzylisocyanate, *p*-nitrobenzenediazonium tetrafluoroborate, dibutyltin dilaurate (DBTDL), and polymethylmethacrylate ( $M_w \sim 120,000$ ,  $T_g = 114$  °C, inherent viscosity 0.2) were purchased from Aldrich Chemical Company. Analytical grade reagents and solvents were used without further purification.

**Synthesis.** Copolymer I (CP I) and copolymer II (CP II) were synthesized by following the literature methods.<sup>13,14</sup>

**4-Methoxyphenyl-4'-(6-methacryloyloxyhexyloxy) benzoate (MMHB) (M-I).** It was synthesized by following the method of Horvath *et al.*<sup>15</sup> using 4-hydroxy benzoic acid as the starting material (Yield, 56%). <sup>1</sup>H NMR (200 MHz, DMSO- $d_6$ ):  $\delta$  (ppm) 8.01 (d, 2H), 7.04 (m, 6H), 5.99 (s, 1H), 5.63 (s, 1H), 4.08 (d, 4H), 3.74 (s, 3H), 1.85 (s, 3H), 1.39-1.72 (m, 8H). Anal. Calcd. for  $C_{24}H_{28}O_6$ : C, 69.89, H, 6.84 Found: C, 69.51, H, 7.19

**4-Nitrophenyl azophenyl-N-methylhexyl methacrylate (NAMM) (M-II).** This monomer was synthesized in three steps by using the method described in literature.<sup>14</sup> 4'-[(6-Hydroxyhexyl)methylamino]-4-nitroazobenzene (HMNA, 5 g, 14.04 mmole) was dissolved with triethylamine (3.55 g, 35.11 mmole) and a trace amount of 1,4-hydroquinone in dried methylene chloride (50 mL). Methacryloyl chloride (3.67 g, 35.11 mmole) was added while stirring at 60 °C for 30 minutes. The reaction mixture was kept stirring at 40 °C for 24 h. The reaction mixture was cooled to room temperature and excess methylene chloride was added. Repeated extraction was carried out in water. The solution was dried over anhydrous sodium sulfate. The solvent was evaporated and the residue was recrystallized from ethanol (Yield, 60%). <sup>1</sup>H NMR (200 MHz, DMSO- $d_6$ ):  $\delta$  (ppm) 8.33 (d, 2H), 7.89 (m, 4H), 6.84 (d, 2H), 5.99 (s, 1H), 5.63 (s, 1H), 4.08 (t, 2H), 3.46 (t, 2H), 3.05 (s, 3H), 1.85 (s, 3H), 1.32-1.57 (m, 8H). Anal. Calcd. for  $C_{23}H_{28}N_4O_4$ : C, 65.08, H, 6.65, N, 13.20 Found: C, 65.43, H, 6.44, N, 13.52.

**2-Methylene-succinic acid bis-(6-{methyl-[4-(4-nitrophenylazo)-phenyl]-amino}-hexyl) ester (MSAE) (M-III).** 4'-[(6-Hydroxyhexyl)methylamino]-4-nitroazobenzene (HMNA) was reacted with itaconic acid using Mitsunobu reaction.<sup>16,17</sup> 3.56 g (0.01 mole) HMNA was dissolved in THF (50 mL). To the solution, 6.55 g (0.025 mole) triphenyl phosphine dissolved in THF (10 mL) was added. The solution was stirred while purging with argon gas at room temperature. A solution containing diisopropyl azodicarboxylate (4.04 g, 0.02 mole) and itaconic acid (0.72 g, 0.055 mole) in 10 mL THF was added dropwise for 40 minutes. The progress of the reaction was checked by thin layer chromatography (TLC). The reaction was completed in 2 h. The solution was cooled in deep freezer and filtered. The residue was recrystallized from acetonitrile to get pure product

(Yield, 70%). <sup>1</sup>H NMR (200 MHz, DMSO- $d_6$ ):  $\delta$  (ppm) 8.34 (d, 4H), 7.93 (m, 8H), 6.85 (d, 4H), 6.23 (s, 1H), 5.73 (s, 1H), 4.06 (m, 6H), 3.50 (m, 4H), 3.11 (s, 4H), 2.87 (s, 2H), 1.39-2.04 (m, 16H). Anal. Calcd. for  $C_{43}H_{50}N_8O_8$ : C, 64.01, H, 6.25, N, 13.89 Found: C, 64.98, H, 6.64, N, 13.11

**Synthesis of Copolymers.** Equimolar mixture of M-I (mesogenic monomer) and M-II was dissolved in freshly distilled N-methyl pyrrolidone (NMP) to a total monomer concentration of 0.4 mole/L. Azobisisobutyronitrile (AIBN) (2 mole % with respect to total monomer) was added to the monomer solution. The solution was taken in a glass ampoule and embedded gas was removed by repeating a vacuum-freeze-thawing technique. The ampoule was placed in oil bath maintained at 70 °C and the solution was kept under stirring for 60 h. The copolymer was precipitated into hot ethanol. The precipitated copolymer was purified by successive reprecipitation from THF into n-hexane. The pure copolymer (CP III) was filtered and dried under reduced pressure at 60 °C for 48 h (Yield, 48%). Copolymer IV was also prepared by the same method.

### Characterization

**NMR Spectroscopy.** Proton NMR spectrum was recorded with Varian 200 NMR spectrometer using tetramethylsilane as an internal standard and dimethylsulfoxide- $d_6$  as a solvent.

**UV/VIS spectroscopic study.** Hewlett Packard (PDA type, model 8453) spectrophotometer was employed to record the UV/VIS spectrum from 190 to 1100 nm. Both copolymer solutions (in THF) and films were used. The films were prepared by spin coating from 2-5% copolymer solution in THF and then, dried under vacuum at 60 °C for 24 h. For studying the photoisomerization of the copolymer, the solutions taken in quartz cell or copolymer films coated on glass slides were placed in the UV/VIS spectrophotometer. The samples were irradiated with a high pressure mercury lamp (intensity 35.6 mW/cm<sup>2</sup>) and the absorption spectra were recorded simultaneously. The spectrum was taken for every 0.5 second. The light intensity reported herein was measured using broadband power/energy meter (model 13PEM001, Melles Griot)

**Gel permeation chromatography.** The number average molecular weight ( $M_n$ ) and molecular weight distributions were determined by using gel permeation chromatography (Waters, model 440) attached with 410 diffraction refractometer. Spectral grade THF was used as a solvent and molecular weight calibration was done using a polystyrene standard.

**Differential Scanning Calorimetry.** Thermal transition temperatures were examined by using differential scanning calorimeter (Perkin Elmer, DSC 4) at a scan rate of 10 °C/min under nitrogen atmosphere. Both heating and cooling scans were repeated three times.

**Optically Induced Birefringence.** The setup for measuring optically induced birefringence is shown in Figure 1, where the change in transmission of the He-Ne laser through

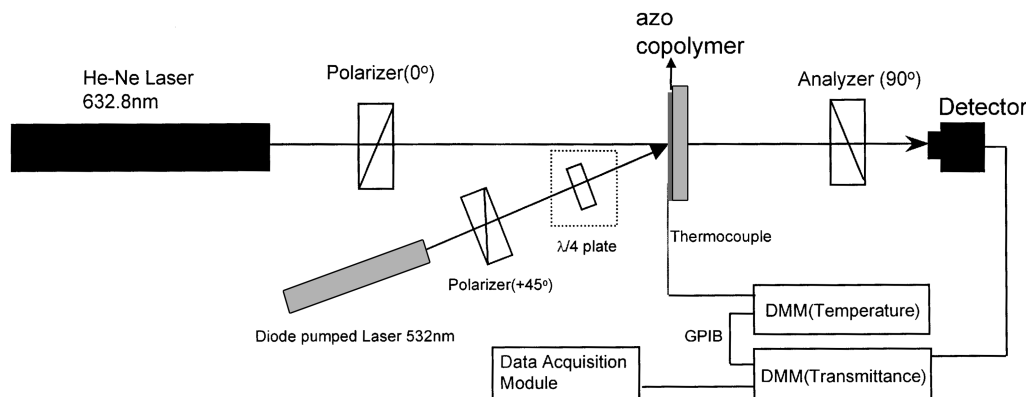


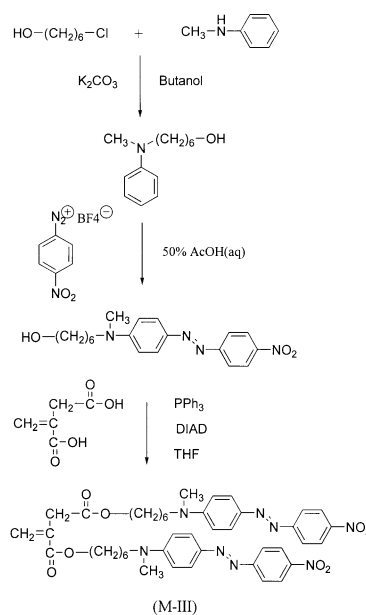
**Figure 1.** Schematic diagram for the measurement of optically induced birefringence.

the film between crossed polarizers is recorded as a function of time after irradiation of pumped diode laser ( $\lambda = 532$  nm, max. intensity  $216 \text{ mW/cm}^2$ ). Under the maximum light intensity, the temperature of the surface of the sample increased by  $5\text{--}6$  °C for measuring period. All the samples underwent identical thermal effect. He-Ne laser ( $\sim 10$  mW) at  $632.8$  nm was used as a probe light to measure the power which is transmitted. Optical anisotropy was induced in the polymer film using a polarized light emitted by pumped diode laser. The wavelength of the pump beam is in the absorption range of the copolymers. To remove the birefringence that had been induced, a quarter waveplate ( $\lambda/4$ ) was inserted into the optical path before the sample. The transmission was detected with a photodiode detector (New Port 818-SL). The transmitted signal  $I(t)$  due to birefringence can be shown to be proportional to  $\sin^2(\pi d \Delta n/\lambda)$  where  $d$  and  $\Delta n$  are thickness and birefringence of the film, respectively.  $\lambda$  is the wavelength of the probe beam (the He-Ne laser radiation at  $632$  nm). We measured the thickness of the films using the surface profilometer (Tencor P10) in order to calculate absolute birefringence ( $\Delta n(t)$ ) using the following Eq. (1).

$$\Delta n(t) = [\lambda/\pi d] \arcsin [(I(t)/I_0)^{0.5}] \quad (1)$$

## Results and Discussion

Synthetic procedure of itaconate monomer is illustrated in Scheme 1. The chemical structures of disperse red 1 and copolymers are also shown in Scheme 2. Four different copolymers were prepared by free radical polymerization method with a small amount of AIBN ( $[M]/[I] = 50$ ). Copolymer I (CP I) was prepared using the methacrylate (M-II) bearing the aminonitro azobenzene and methylmethacrylate (MMA). Copolymer II (CP II) was also prepared using the  $\alpha$ -methylstyrene containing an aminonitro azobenzene and MMA. Copolymer III (CP III) consists of MMHB (M-I) and NAMM (M-II) units, whereas copolymer IV (CP IV) consists of MMHB (M-I) and MSME (M-III) units. All the copolymers are red in color and well soluble in organic solvents such as tetrahydrofuran, dimethylformamide, chloroform, acetone etc. Composition ratio of each copolymer was determined by NMR and elemental analysis. The details

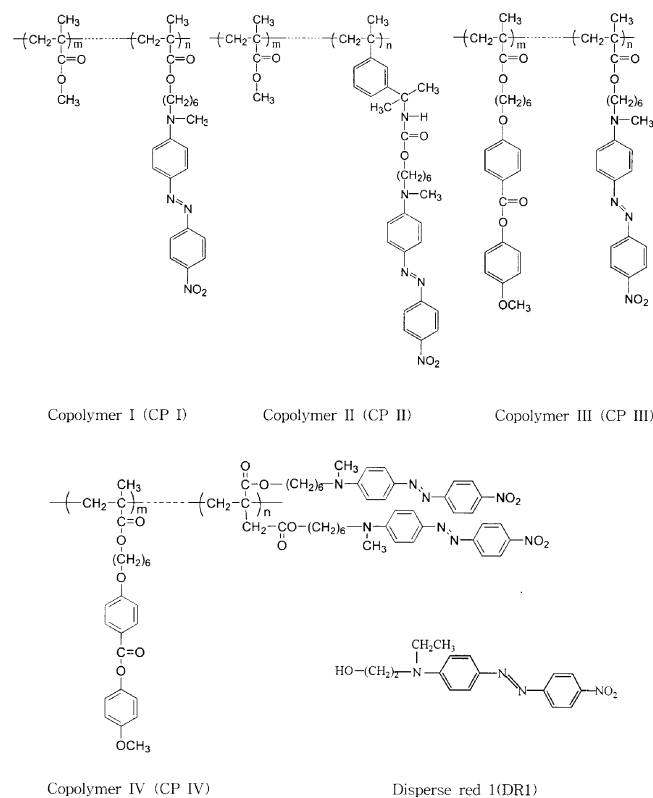


**Scheme 1.** Synthetic procedure for itaconate monomer (M-III).

about monomer feeding ratio, copolymer composition, molecular weight, and glass transition temperature are listed in Table 1.

In DSC thermogram, CP III shows the monotropic liquid crystalline (LC) transition behavior when heating the sample. In the meanwhile CP IV shows the amphotropic LC transition behavior when heating and cooling in both ways. The textures were confirmed to be nematic in copolymers by polarized optical microscopy. The thin films were obtained by dissolving the copolymers in THF and casting onto a clean glass slide. We dried the films thoroughly at room temperature under vacuum for 48 h. Intrinsic birefringence of liquid crystalline copolymers was extremely small to be negligible.

**Photoisomerization behavior.** All the azo monomers and copolymers were found to undergo isomerization in both solution and film states under UV irradiation. In Figure 2, the representative UV-VIS spectrum of CP I was shown to observe the absorption behavior of the azo chromophore and the absorption maximum was found at  $463$  nm, which



**Scheme 2.** Structures of copolymers and disperse red 1 used in this study.

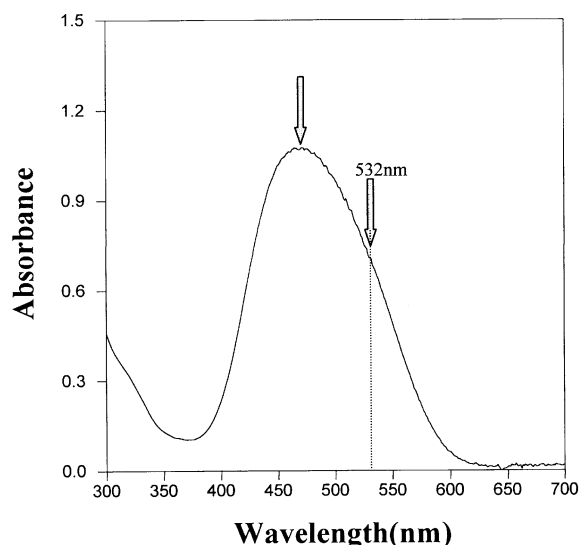


**Figure 2.** UV-VIS absorption spectrum of copolymer I (CP I).

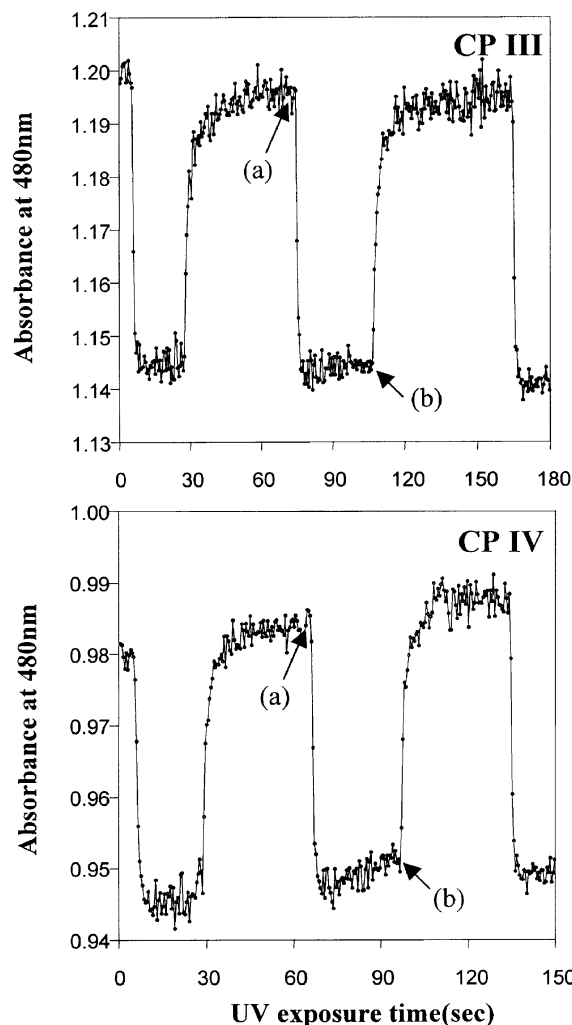


**Figure 3.** Change of the absorbance at 480 nm under UV exposure. (a) UV light on and (b) UV light off.

can be assigned to  $\pi - \pi^*$  transition in azobenzene unit. Cut-off wavelength was found around 630 nm. The wavelength of the excitation light (532 nm) is in the range of the absorption. We selected CP III and CP IV to fabricate the thin films on the glass slide. UV-VIS spectroscopy was used to monitor high-speed *trans-to-cis* and *cis-to-trans* isomerization behavior of the copolymer films. Measurements were performed with HP 8453 Spectrophotometer and the sample was exposed to the light from a high pressure Mercury lamp fitted through a flexible liquid optic fiber. All studies were conducted using unfiltered UV light at an intensity of 35.6 mW/cm<sup>2</sup>. The conversion from *trans* to *cis* form was moni-

**Table 1.** Molar composition, molecular weight, polydispersity, and the glass transition temperature of synthesized each copolymer

	Monomer Feeding Mole Ratio		Resultant Mole Composition		Molecular Weight (M <sub>n</sub> )	Polydispersity	Glass Transition Temperature (°C)
	A	B	A	B			
CP I	1	1.5	1	0.7	9317	2.9017	115.0
CP II	1	2	1	1	10027	2.1041	118.0
CP III	1	1	1	0.9	7012	2.2357	56.0
CP IV	1	1	1	0.4	5328	2.5034	37.5

tored by following the decrease in the intensity of 480 nm absorption band upon exposure as a function of time. In Figure 3, we recorded the change of the absorbance at 480 nm in the cases of CP III and CP IV. When the absorbance reached to the minimum value, we close the shutter to monitor the increase of the absorbance again. The absorbance ( $\pi - \pi^*$  transition) at 480 nm is reduced during UV irradiation, as trans form gradually isomerizes to cis form. The change of the absorbance at 480 nm was observed to be quite reversible.

**Dynamic behavior of photoinduced birefringence.** A typical sequence for inducing birefringence and relaxation in four kinds of copolymers are presented in Figure 4, 6, 7, 8, and 9 including that in PMMA doped with disperse red 1 (DR1).

The film was fabricated with spin coater at the speed (2000 rpm) using the solution whose concentration is 5 wt%. The thicknesses of the samples were measured to be around 0.2-0.3  $\mu\text{m}$ . No transmission of the probe beam is detected through the crossed polarizers. Optical anisotropy is induced by exposure to a linearly polarized pumped diode laser beam ( $\lambda = 532 \text{ nm}$ ). The excitation beam is polarized at  $45^\circ$  with respect to the polarizer axis. When optical anisotropy is induced in the polymer film, the probe light is partially transmitted through the optical setup and transmission reaches to the maximum level. At the second stage, the excitation light is turned off and the transmission was observed to decrease to a certain level. This shows that the induced optical anisotropy is not completely retained after excitation with a linearly polarized light. When we insert the quarter waveplate in front of the sample, the excitation light was changed to circularly polarized light. Under the exposure to circularly polarized light, the induced birefringence vanished at all, arising from randomization of oriented polar azobenzene molecules.

In analyzing the growth of birefringence, the fast mode

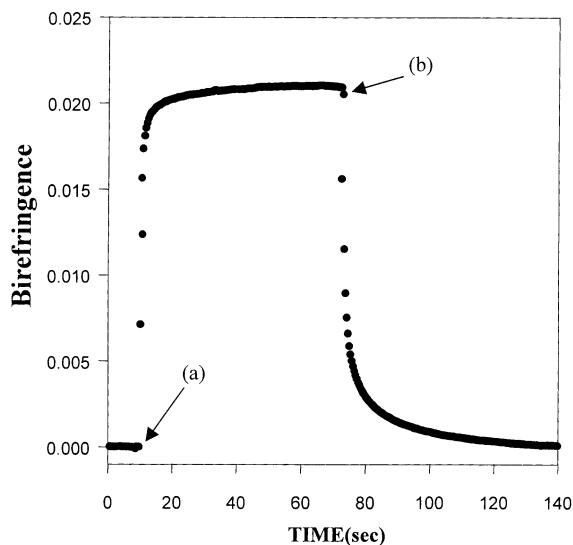


**Figure 4.** Growth and decay of birefringence on a PMMA/5 wt% DR1 film. (a) The writing beam is turned on and (b) The writing beam is turned off. \*Pump beam intensity 216 mW/cm<sup>2</sup>.

and the slow mode can be classified. The fast mode of growth is mainly attributed to the reorientation of azobenzene molecules forced by side chain mobility and the slow mode is partly due to the main chain motion.<sup>18</sup> In the decay of birefringence, the fast and slow modes are all attributable to the inherent properties of polymers.

### 1. Photoinduced birefringence of guest-host system:

We prepared the mixed solution of polymethylmethacrylate and disperse red 1 (DR1, 5 wt%). At the beginning of the experiment, it was found that no light is transmitted through the optic setup as the azo molecules are randomly oriented in the polymer matrix. As the polarized pump light (intensity 216 mW/cm<sup>2</sup>) is irradiated on the surface of the sample, an anisotropic orientational distribution of azobenzene group is created as a result of the accumulation of the cis isomers and of trans isomers that are oriented with the transition dipole ( $\Delta\mu$ ) perpendicular to the polarization vector of the pump beam. Light is thus transmitted through the analyzer due to the onset of the birefringence. When the excitation light is turned off, the signal starts to decay back to the zero level. In the guest-host system, this decay is rapid and system reverts to equilibrium in a short period. The dynamic behavior of birefringence is shown in Figure 4. Using the measured thickness, we could calculate the birefringence with transmission.

Dynamic properties of growth and decay of the birefringence were investigated after curve fitting the birefringence data to the double exponential rising and decaying functions (equation (2), (3)). As shown in Figure 4, both the growth and decay are very fast in many cycles. The maximum birefringence can be achieved within 6 seconds under the setting intensity of excitation light. The birefringence fell down to 67% of the maximum signal within 2 seconds after blocking the light. This is the typical characteristic in guest-host system although the glass transition temperature of PMMA is around 114 °C. Guest polar azobenzene molecules are not tethered and free to reorient perpendicular to the polarization direction of the excitation beam. Then oriented azo molecules are totally converted to random orientation without excitation light because the motion of DR1 molecules is not

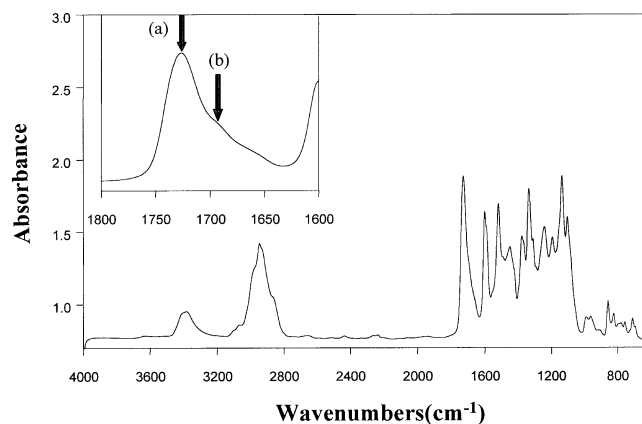


**Figure 5.** Infrared spectrum of copolymer II (CP II). (a) isolated mode of carbonyl stretching and (b) hydrogen bonded mode of carbonyl stretching.

restricted in the PMMA matrix physically or chemically.

$$\text{Growth: } \Delta n(t) = A [1 - \exp(-k_1 t)] + B [1 - \exp(-k_2 t)] \quad (2)$$

$$\text{Decay: } \Delta n(t) = C \exp(-k_3 t) + D \exp(-k_4 t) + R \quad (3)$$

In the rising curve,  $k_1$  and  $k_2$  were calculated to be 1.6227 and 0.0022/sec respectively. Fast process is predominant in the growth of birefringence, which can be ascribed to the motion of guest molecules totally. Decaying process was also very fast and no residual birefringence was observed in 50 seconds. As can be seen in Table II, the rate constants,  $k_1$ ,  $k_3$ , and  $k_4$  are the largest compared to those of other polymers.

**2. Photoinduced birefringence of CP I and CP II:** CP I is composed of methacrylate backbone whereas CP II is composed of two different repeating units that are  $\alpha$ -methylstyrene and methylmethacrylate. In CP II, carbamate group is placed in the side chain to anchor the polar azobenzene group to the polymer backbone. Hydrogen bond exists between the hydrogen in secondary amine and oxygen in carbonyl group, which can be observed in infrared spectrum of CP II. (see Figure 5) The isolated and the hydrogen bonded mode of carbonyl stretching band were assigned to 1725 and 1698  $\text{cm}^{-1}$ , respectively. We can also observe combined band around 3409-3348  $\text{cm}^{-1}$ . The NH stretching band can be divided into two modes such as isolated mode at 3409  $\text{cm}^{-1}$  and hydrogen bonded mode at 3348  $\text{cm}^{-1}$ . The calculated fraction of hydrogen bonded carbonyl stretching was about 56.2%, which was curve resolved on the basis of Gaussian function. The azobenzene moiety in CP II is more geometrically hindered than that in CP I resulting from the hydrogen bond between the side chain themselves. The molar composition of the azobenzene moieties in CP I and CP II are 41.0% and 52.5%, respectively. The glass transition temperatures of the two polymers are almost identical

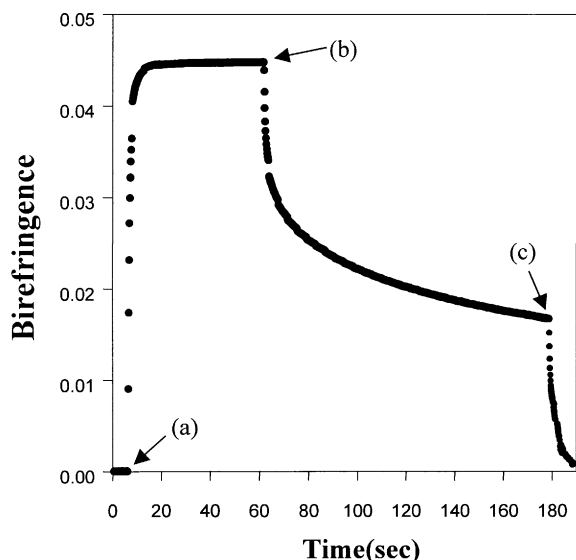


**Figure 6.** Growth and decay of birefringence on a copolymer I (CP I) film. (a) The writing beam is turned on, (b) The writing beam is turned off, and (c) Circularly polarized light on. \*Pump beam intensity 216  $\text{mW}/\text{cm}^2$ .

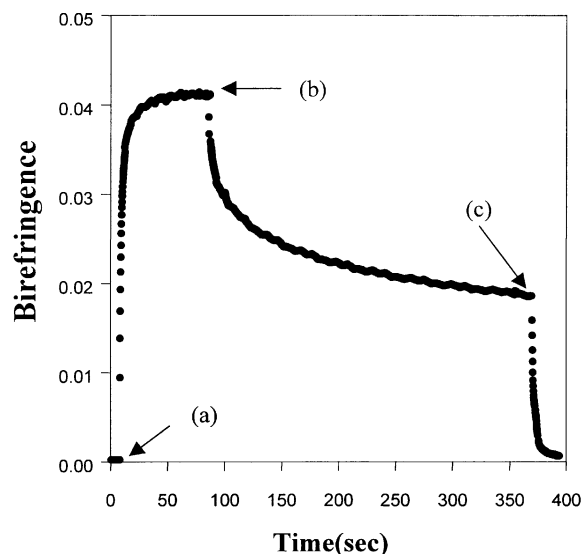


**Figure 7.** Growth and decay of birefringence on a copolymer II (CP II) film. (a) The writing beam is turned on, (b) The writing beam is turned off, and (c) Circularly polarized light on. \*Pump beam intensity 216  $\text{mW}/\text{cm}^2$ .

(CP I, 115  $^{\circ}\text{C}$ ; CP II, 118  $^{\circ}\text{C}$ ). The maximum birefringence is almost same to be 0.043-0.044 although the density of the azobenzene moiety is higher than that in CP I. This implies that the hydrogen bond interrupts the reorientation of the polar azobenzene moieties under the linearly polarized light. When we irradiate the sample with the pump beam, the birefringence signal rises very rapidly and the relaxation behavior is also quite fast. (See Figure 6 and 7) Under the same intensity of excitation light (intensity 216  $\text{mW}/\text{cm}^2$ ), rate constants in CP I are larger than those in CP II. As the growth of birefringence in CP I is much faster, the decay of birefringence is also much faster than that in CP II. Shortly, the dynamic property in photoinduced birefringence is affected by hydrogen bonds between the side chains. It can retard the speed of growth and decay of optically induced birefringence.

**3. Photoinduced birefringence of CP III and CP IV:** The induced birefringences of CP III and CP IV were plotted with the change of the irradiation time in Figure 8 and Figure 9, respectively. When we irradiate with the pump beam whose intensity is 216  $\text{mW}/\text{cm}^2$ , the growth of birefringence in CP III is faster than that of CP IV. (See Table 2) This behavior can be explained in terms of difference of polymer structure. Compared with CP III, CP IV has two polar azobenzene moieties in one repeating unit. Inherently, it can be thought that the dipolar interaction between polar azobenzene moieties in CP IV is larger than that in CP III. An antiparallel association of neighboring dipoles is much more favorable in CP IV. The vicinal dipoles in the side chain are oriented preferentially antiparallel to each other and the electric field of the neighboring dipoles reduced the mobility of the azo group.<sup>11</sup>

Therefore, it is much harder to disorganize the antiparallel arrangement of polar azo molecules in CP IV. This structural factor retards the rate of growth and decay of birefringence.

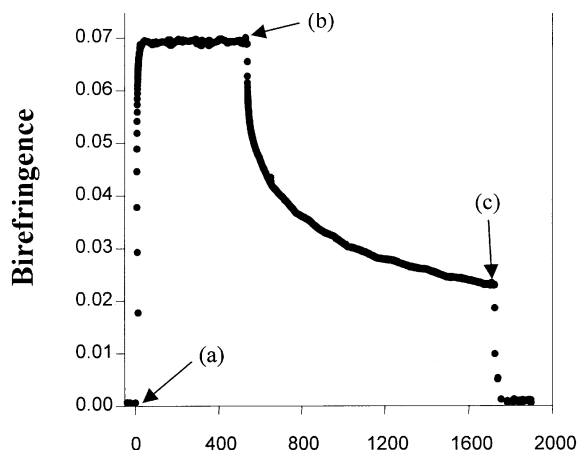


**Figure 8.** Growth and decay of birefringence on a copolymer III (CP III) film. (a) The writing beam is turned on, (b) The writing beam is turned off, and (c) Circularly polarized light on. \*Pump beam intensity  $216 \text{ mW/cm}^2$ .

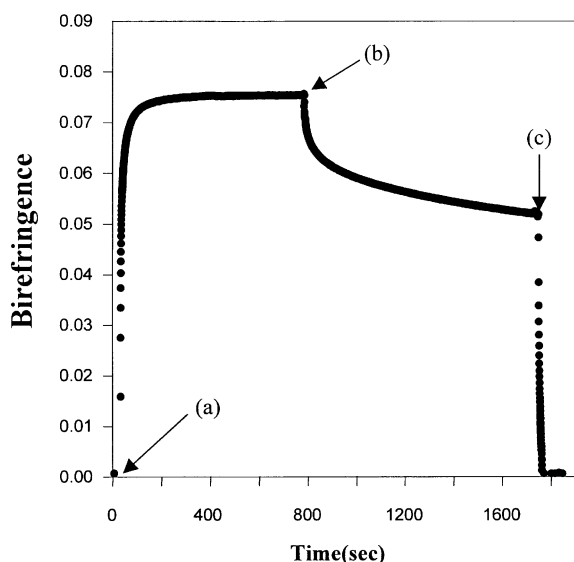


**Figure 9.** Growth and decay of birefringence on a copolymer IV (CP IV) film. (a) The writing beam is turned on, (b) The writing beam is turned off, and (c) Circularly polarized light on. \*Pump beam intensity  $216 \text{ mW/cm}^2$ .

We varied the intensity of pump beam to investigate the effect on the value of birefringence and kinetic parameters in the growth and the decay of birefringence. The higher birefringence value was observed under the higher intensity of excitation light. (see Figure 10) In the case of CP IV, the birefringence was obtained after 800 sec irradiation because it did not reach the maximum level in 2,000 seconds. This indicates that larger number of reoriented azobenzene molecules was involved in the local ordering to induce the optical anisotropy. As we recognize,  $k_1$  and  $k_2$  values decreases as the intensity increases. The increasing effect on  $k_1$  is much more severe than that on  $k_2$ . In the fast process of growth, the value of  $k_1$  increased as the beam intensity increased. However, in the fast process of decay, the value of  $k_3$  does not show significant difference with the change of beam intensity (see Figure 11 and 12). This implies that the relaxation

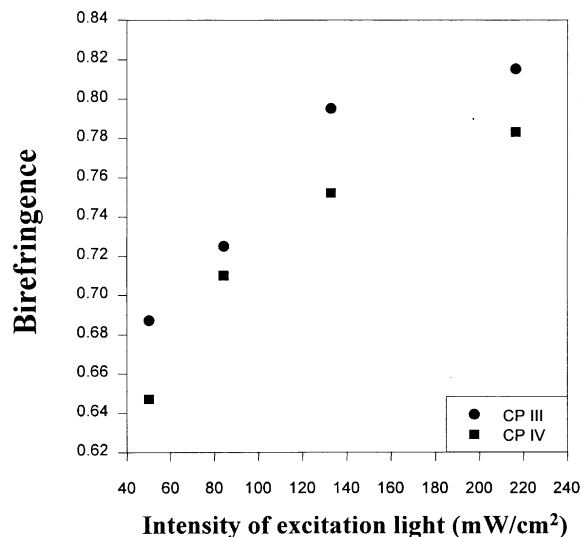


**Figure 10.** Relationship between the intensity of excitation light and birefringence in copolymer III and IV.

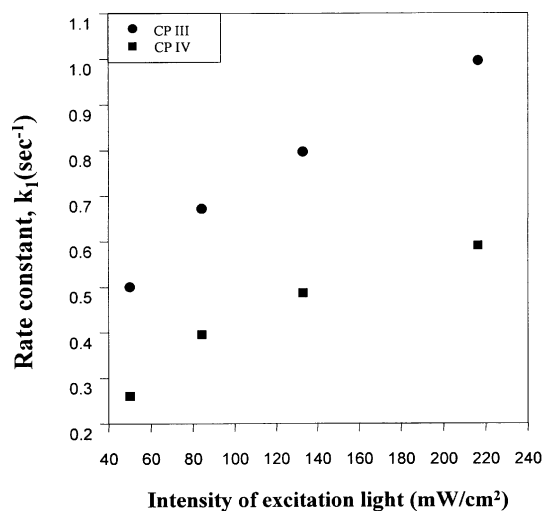


**Figure 11.** Relationship between the intensity of excitation light and growth rate constant,  $k_1$  in copolymer III and IV.

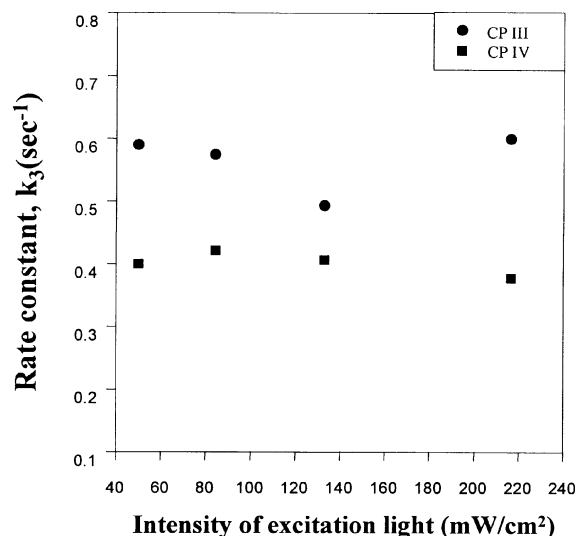


**Figure 12.** Relationship between the intensity of excitation light and decaying rate constant,  $k_3$  in copolymer III and IV.

of birefringence is strongly dependent on the intrinsic properties of copolymers, which can be driven only by thermal mode.

**4. Comparison of photoinduced birefringence between amorphous copolymers (CP I, CP II) and liquid crystalline copolymer (CP III, CP IV):** Resulting from the DSC thermal analysis, the glass transition temperatures of CP I and CP II were observed to be much higher than those of CP III and CP IV. (See Table 1) Although CP III is monotropic and CP IV is amphotropic, no inherent birefringence was detected at room temperature in this experiment. It is important to know how fast the birefringence grows and decays and what level of birefringence would be stable for a long time.

In many literatures, decaying process is reported to be affected by the inherent thermal property of polymer. In the case of the polymer that shows high  $T_g$ , the birefringence relaxation is highly retarded due to the main chain rigidity accompanying with the retarded motion of the side chain. Although the amorphous copolymers showed much higher  $T_g$  than the other two, the relaxation process was found much faster than those in CP III and CP IV. The only difference between these two classes of copolymer is that the latter (CP III & CP IV) contains a mesogenic group through a flexible methylene spacer in the side chain of the copolymer. Those mesogenic groups are placed in the vicinity of polar azobenzene moieties, which can be mutually interactive geometrically. Therefore, the growth of birefringence in CP III and CP IV is slower than that in CP I and CP II. (See Table 2) This is strongly ascribed to the more free volume close to polar azobenzene moieties in CP I and CP II because methylmethacrylate is less bulky than the mesogenic side chain group in CP III and CP IV.

In the relaxation process of birefringence in CP III and CP IV, polar azobenzene molecules reoriented with cooperative motion of mesogenic group was found much harder to be randomized due to steric hindrance, dipole-dipole interaction, van der Waals interaction etc. Using the theoretical calculation with HYPER CHEM 5.0, we calculated dipole moment in the ground state using semiempirical method (AM1).

Comonomer (M-I) with mesogenic group has 3.43 debye of dipole moment, which shows relatively weak polarity. However, the mesogenic comonomer can induce the dipole-dipole interaction with polar azobenzene moieties. In the cases of CP I and CP II, azobenzene molecules were reoriented under an excitation light and randomized to the isotropic state for themselves more easily. However, once the azobenzene molecules reorient to be perpendicular to the polarization direction of the excitation light, the bulky mesogenic group tends to associate to move to the same direction of azobenzene molecules in the cases of CP III and CP IV. Therefore, the activation energy of the latter is likely to be higher than those in CP I and CP II. Shortly, reorientation of the azobenzene moieties did influence the neighboring mesogenic group even when the film was below  $T_g$  of the copolymers (CP III and CP IV).

Resulting from above all the experiments, high  $T_g$  polymer does not always show better stability of birefringence than lower  $T_g$  polymer does at room temperature. There are many factors to affect the rising and decaying process of birefringence. The residual birefringence and rate of relaxation can be attributed to the environmental free volume and steric hindrance of azobenzene molecule imposed by dipolar interaction and van der Waals interaction.

## Conclusion

We synthesized four different types of copolymer bearing an aminonitro azobenzene chromophore in the side chain. Aminonitro azobenzene was synthesized to be introduced to side chain copolymers through the flexible methylene spacers. All copolymers contain aminonitroazobenzene molecules in the side chain. Trans-to-cis photoisomerization was clarified under the exposure of UV light with the UV-VIS absorption spectroscopy. Optical anisotropy can be induced under exposure to a linearly polarized light at 532 nm. The dynamics of photoinduced birefringence let us compare the effect of polymeric structure on the rate of growth and decay of the birefringence. The dipolar interaction of azobenzene molecules and cooperative motion of environmental molecules in

**Table 2.** Parameters obtained by fitting the birefringence data to equation (2) and (3). Experiments were performed at room temperature

	Intensity of Pump Beam (mW/cm <sup>2</sup> )	A	B	$k_1$ (/sec)	$k_2$ (/sec)	C	D	$k_3$ (/sec)	$k_4$ (/sec)	R
PMMA/5 wt% DR1	216.5	0.0254	0.0125	1.6227	0.0022	0.0176	0.0047	0.9519	0.0668	0.0056
CP I	216.5	0.0567	0.0108	1.2391	0.0986	0.0115	0.0166	0.8444	0.0429	0.0196
CP II	216.5	0.0260	0.0134	0.9014	0.0710	0.0062	0.0098	0.6910	0.328	0.0238
CP III	216.5	0.0546	0.0124	0.9960	0.0708	0.0088	0.0118	0.5998	0.0248	0.0459
(methacrylate Copolymer)	132.9	0.0509	0.0250	0.7967	0.0843	0.0094	0.0167	0.4933	0.0186	0.0516
	84.3	0.0353	0.0315	0.6720	0.1047	0.0054	0.0083	0.5743	0.0492	0.0588
	50.0	0.0317	0.0420	0.5010	0.1315	0.0095	0.0099	0.5902	0.0319	0.0616
CP IV	216.5	0.0485	0.0244	0.5898	0.0523	0.0054	0.0089	0.3775	0.0210	0.0608
(Itaconate Copolymer)	132.9	0.0298	0.0309	0.4862	0.0373	0.0069	0.0086	0.4062	0.0373	0.0546
	84.3	0.0328	0.0352	0.3949	0.0326	0.0056	0.0085	0.4216	0.0225	0.0684
	50.0	0.0307	0.0396	0.2612	0.0277	0.0063	0.0088	0.4017	0.0198	0.0599



the vicinity of azobenzene molecules are found to be important factor to affect the rate of relaxation and the stability of birefringence.

**Acknowledgment.** This work was supported by Korea Science and Engineering Foundation (contract#: 96-0300-10-03-3) and Kyung Hee University(1999).

### References

1. Ikeda, T.; Horiuchi, S.; Karanjit, D. B.; Kurihara, S.; Tazuke, S. *Macromolecules* **1990**, *23*, 42.
  2. Chen, C.; Dalton, L.; Yu, L.; Shi, Y.; Steier, W. *Macromolecules* **1992**, *25*, 4032.
  3. Ringsdorf, H.; Schmidt, H-W. *Makromol. Chem.* **1984**, *185*, 1327.
  4. Pham, V. P.; Galstyan, T.; Granger, A.; Lessard, R. A. *Jpn. J. Appl. Phys.*, Part 1, No. 1B **1997**, *36*, 429.
  5. Rochon, P.; Gosselin, J.; Natansohn, A.; Xie, S. *Appl. Phys. Lett.* **1992**, *60*(1), 6.
  6. Eich, M.; Wendorff, J. H.; Reck, B.; Ringsdorf, H. *Makromol. Chem., Rapid Comm.* **1987**, *8*, 59.
  7. Natansohn, A.; Xie, S.; Rochon, P. *Macromolecules* **1992**, *25*, 5531.
  8. Natansohn, A.; Rochon, P.; Gosselin, J.; Xie, S. *Macromolecules* **1992**, *25*, 2268.
  9. Rochon, P.; Bissonnette, D.; Natansohn, A.; Xie, S. *Applied Optics* **1993**, *32*(35), 7277.
  10. Natansohn, A.; Rochon, P.; Pezolet, M.; Audet, P.; Brown, D.; To, S. *Macromolecules* **1994**, *27*(9), 2580.
  11. Brown, D.; Natansohn, A.; Rochon, P. *Macromolecules* **1995**, *28*, 6116.
  12. Natansohn, A.; Rochon, P.; Ho, M. S.; Barrett, C. *Macromolecules* **1995**, *28*, 4179.
  13. Ahn, J. S.; Choi, D. H.; Rhee, T. H.; Kim, N. *Polymer (Korea)* 1998, *22*(1), 150.
  14. Robello, D. R. *J. Polym. Sci., Part A Chem. Ed.* **1990**, *28*, 1.
  15. Horvath, J.; Nyitrai, K.; Cser, F.; Hardy, G. Y. *Eur. Polym. J.* **1985**, *21*(3), 251.
  16. Pautard, A. M.; Evans, Jr. S. A. *J. Org. Chem.* **1988**, *53*, 2300.
  17. Roush, W. R.; Blizzard, T. A. *J. Org. Chem.* **1984**, *49*, 4332.
  18. Ho, M. S.; Natansohn, A.; Barrett, C.; Rochon, P. *Can. J. Chem.* **1995**, *73*, 1773.
-